ISSN 1063-7761, Journal of Experimental and Theoretical Physics, 2013, Vol. 117, No. 6, pp. 988–998. © Pleiades Publishing, Inc., 2013.
Original Russian Text © S.Ya. Vetrov, R.G. Bikbaev, I.V. Timofeev, 2013, published in Zhurnal Eksperimental'noi i Teoreticheskoi Fiziki, 2013, Vol. 144, No. 6, pp. 1129–1139.

ATOMS, MOLECULES, OPTICS

Optical Tamm States at the Interface between a Photonic Crystal and a Nanocomposite with Resonance Dispersion

S. Ya. Vetrov[a,b], R. G. Bikbaev[a,*], and I. V. Timofeev[a,b]

[a] *Siberian Federal University, Svobodnyi pr. 79, Krasnoyarsk, 660041 Russia*

* *e-mail: rashid-bikbaev@mail.ru*

[b] *Kirensky Institute of Physics, Siberian Branch, Russian Academy of Sciences, Akademgorodok, Krasnoyarsk, 660036 Russia*

Received May 7, 2013

Abstract—Optical Tamm states localized at the edges of a photonic crystal bounded from one or both sides by a nanocomposite have been studied. The nanocomposite consists of metallic nanoinclusions, which have a spherical or orientationally ordered spheroidal shape and are dispersed in a transparent matrix, and is characterized by the resonant effective permittivity. The transmission, reflection, and absorption spectra have been calculated for waves with longitudinal and transverse polarizations in such structures at the normal incidence of light. The spectral manifestation of Tamm states that is due to the existence of negative values of the real part of the effective permittivity has been analyzed for the visible spectral range. It has been established that the characteristics of Tamm states localized at the edge of the photonic crystal depend strongly both on the concentration of nanoballs in the nanocomposite film and on its thickness. Modes formed by two coupled Tamm plasmon polaritons localized at the edges of the photonic crystal adjacent to two nanocomposite layers have been examined. It has been shown that, in the case of the anisotropic nanocomposite layer adjacent to the photonic crystal, each of two orthogonal polarizations of the incident wave corresponds to a specific frequency of the Tamm state localized at the edge; owing to this property, the transmission spectra of such a structure are polarization sensitive.

DOI: 10.1134/S1063776113140185

1. INTRODUCTION

Materials with photonic band gaps in their energy spectrum are called photonic crystals and constitute a new class of materials for photonics and optoelectronics whose dielectric properties vary periodically with a period allowing the Bragg diffraction of light. The theory of propagation of electromagnetic radiation in periodic media has a very close formal similarity to the quantum theory of electrons in crystals. The band structure of the energy spectrum of electrons, which is due to the Bragg reflection of electrons, is similar to the band structure of the photonic crystal. The presence of photonic band gaps and regions of an anomalous increase in the photon density of states provides the possibility of the efficient control of the characteristics of laser radiation [1–4]. An advance has been achieved in the solution of fundamental problems concerning, e.g., the control of the processes of spontaneous emission of light from atoms and molecules, as well as the localization and channeling of light. Structures with photonic band gaps are widely applied for the creation of photonic crystal waveguides, resonators, and nonlinear optical converters.

In addition to the investigation of the bulk properties of a one-dimensional photonic crystal, which consists of alternating layers of two materials, surface electromagnetic waves at the interface between two photonic crystals, as well as at the interface between the photonic crystal and an isotropic medium with negative permittivity $\varepsilon < 0$, are actively studied [5]. A surface electromagnetic wave at the interface between the photonic crystal and the medium with $\varepsilon < 0$ is certainly coupled to a surface plasmon, i.e., oscillations of free electrons near the surface of the conductor. Such a coupled mode of the radiation field and surface plasmon is called plasmon polariton, which is widely used to analyze surfaces in the visible and infrared spectral ranges.

In addition to the propagating surface waves at the interface of two photonic crystals or the interface between the photonic crystal and the medium with $\varepsilon < 0$, a state in the form of a standing surface wave, which has zero wavenumber and does not transfer energy, can be obtained; such a state can be observed at the normal incidence of waves to photonic crystal layers [5]. Maxwell's equation for the electric field in this case is an exact analog of the single-electron Schrödinger equation for a semi-infinite crystal whose solution is a Tamm surface state. In view of this circumstance, the electromagnetic analog of the elec-

tronic Tamm state is called the optical Tamm state or, in other words, the Tamm plasmon polariton.

Interest in the discovered phenomenon of the extremely high transmission of light through single subwavelength apertures in the metal film has been recently increased [6]. Such an anomalously high transmission of light is due to numerous factors the main of which is the excitation of surface plasmon oscillations [7]. The authors of [8] proposed and implemented for the first time a new mechanism of the extremely high transmission of light through a nanoaperture, which is based on the placing of a gold film with the nanoaperture into a light field localized at the interface between the film and one-dimensional photonic crystal. Additional detailed investigation of the effect of anomalous transmission of light through a nanoaperture whose diameter is much shorter than the wavelength of light in the field of a microcavity formed by a one-dimensional photonic crystal and a gold film was performed in [9]. The numerical simulation in [10] indicates that the effect of anomalously high transmission of light through the nanoaperture that was experimentally observed in [8, 9], is attributed to the enhancement of the field at the interface between the photonic crystal and metal film, which is due to the appearance of an optical Tamm state. Such, the optical Tamm state allows the implementation of a physically interesting transmission regime of light waves through the nanoaperture in the metal film. It was proposed to use the optical Tamm state in applications such as gauges and resonant optical filters [11], optical switchers [12], Faraday rotation amplifiers [13], multichannel filters [14], and fabrication of polariton lasers [15]. A new type of waveguide modes that are formed by two coupled plasmon polaritons was examined in [16]. Additional possibilities of the control of light appear in photonic crystals with the inclusion of nanostructured metal–insulator materials [17–21].

In this work, we demonstrate the possibility of the implementation of the optical Tamm state localized at the edges of the one-dimensional photonic crystal bounded from one or both sides by isotropic or anisotropic metal–insulator nanocomposite media. The nanocomposite consists of metallic nanoparticles dispersed in a transparent matrix and is characterized by the resonant effective permittivity $\varepsilon_{mix}(\omega)$, whereas the optical characteristics of the initial materials have no resonant features [22, 23]. The position of the frequency range where the nanocomposite is similar to a metal, i.e., where $\mathrm{Re}\,\varepsilon_{max}(\omega) < 0$, depends on the permittivities of initial materials, concentration and shape of nanoparticles, which opens wide possibilities of the control of optical properties of the optical Tamm state by means of the variation of the parameters of the nanocomposite. The properties of the optical Tamm state at the interface between the photonic crystal and nanocomposite are compared to those of the optical Tamm state at the interface between the photonic crystal and metal layers.

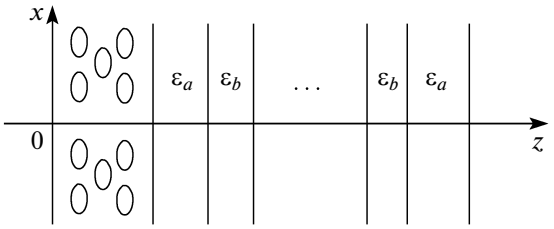

Fig. 1. Layout of the one-dimensional photonic crystal adjacent to the anisotropic nanocomposite layer.

2. DESCRIPTION OF THE MODEL AND DEFINITION OF TRANSMISSION

We consider the photonic crystal structure that is a layered medium bounded from one or both sides by finite nanocomposite media (Fig. 1). A unit cell of the photonic crystal is formed from layers of materials a and b with the thicknesses d_a and d_b and relative permittivities ε_a and ε_b, respectively. The nanocomposite layer with the thickness d_{mix} consists of spheroidal metallic nanoparticles that are uniformly distributed in a dielectric matrix and are oriented along the axis of revolution, which is chosen as the x axis.

Below, we assume that the photonic crystal structure is located in vacuum. The effective permittivity of the nanocomposite with the properties of a uniaxial body in the principal axes has the form of a diagonal tensor with the components $\varepsilon_{xx} = \varepsilon_{\parallel}$ and $\varepsilon_{yy} = \varepsilon_{zz} = \varepsilon_{\perp}$. In the Maxwell–Garnett model, the effective permittivities are given by the expression [23, 24]

$$\varepsilon_{\square,\parallel} = \varepsilon_d\left[1 + \frac{f(\varepsilon_m - \varepsilon_d)}{\varepsilon_d + (1-f)(\varepsilon_m - \varepsilon_d)L_{\square,\parallel}}\right], \qquad (1)$$

where f is the filling factor, i.e., the fraction of nanoparticles in the matrix; ε_d and $\varepsilon_m(\omega)$ are the permittivities of the matrix and metal from which nanoparticles are made, respectively; ω is the radiation frequency; and $L_{\perp,\parallel}$ are the depolarization coefficients depending on the ratio of the lengths of the polar, a, and equatorial, b, semiaxes of an spheroid and on the field direction. For the fields parallel and perpendicular to the axis of revolution of the spheroid,

$$L_{\parallel} = \frac{1}{1-\xi^2}\left(1 - \xi\frac{\arcsin\sqrt{1-\xi^2}}{\sqrt{1-\xi^2}}\right), \qquad (2)$$

where $\xi = a/b$,

$$L_{\square} = (1 - L_{\parallel})/2, \qquad (3)$$

respectively. The cases $\xi < 1$ and $\xi > 1$ correspond to the oblate and prolate spheroids, respectively. The case

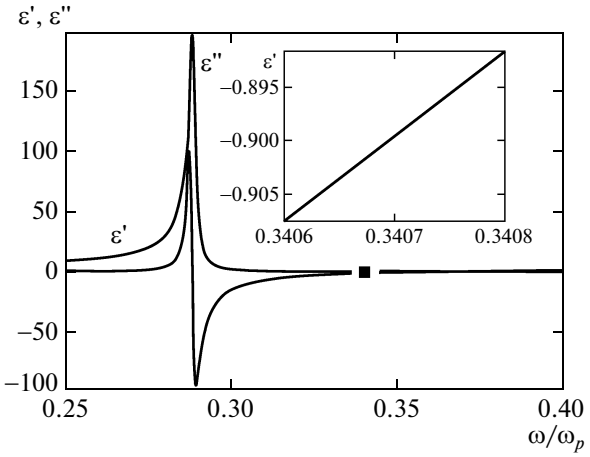

Fig. 2. Imaginary, $\varepsilon''_{mix}(\omega)$, and real, $\varepsilon'_{mix}(\omega)$, parts of the effective permittivity $\varepsilon_{mix}(\omega)$ versus the normalized frequency ω/ω_p. The filling factor is $f = 0.2$. The inset shows $\varepsilon'_{mix}(\omega)$ near the frequency corresponding to the Tamm state in an increased scale (see Fig. 3).

$\xi = 1$, for which $L_\perp = L_\parallel = 1/3$ and $\varepsilon_\perp = \varepsilon_\parallel = \varepsilon_{mix}$, corresponds to the ball.

In the Drude approximation, the permittivity of the metal from which nanoparticles are made has the form

$$\varepsilon_m(\omega) = \varepsilon_0 - \frac{\omega_p^2}{\omega(\omega + i\gamma)}, \quad (4)$$

where ε_0 is a constant presenting the contributions of interband transitions of bound electrons, ω_p is the plasma frequency, and γ is the inverse relaxation time of electrons.

To calculate the transmission of a plane light wave, which is polarized along the x axis and propagates in the z direction, we used the transfer matrix method [25]. Variation of the light field at passage through each layer of the structure is determined by the second-order transfer matrix, and the transfer matrix of the entire structure, which relates the amplitudes of the input and output waves, is the product of such 2×2 matrices,

$$M = T_{01}T_{12}\ldots T_{N-1,N}T_{N,S}, \quad (5)$$

where an individual transfer matrix has the form

$$T_{n-1,n} = \frac{1}{2}\begin{pmatrix} (1+h)e^{-i\alpha_n\gamma_n} & (1-h)e^{i\alpha_n\gamma_n} \\ (1-h)e^{-i\alpha_n\gamma_n} & (1+h)e^{i\alpha_n\gamma_n} \end{pmatrix}. \quad (6)$$

Here, $h = \sqrt{\varepsilon_n/\varepsilon_{n-1}}$; $\varepsilon(n)$ is the permittivity of the nth layer; $\alpha_n = (\omega/c)\sqrt{\varepsilon(n)}$; ω is the frequency of the wave; c is the speed of light; $\gamma_n = z_n - z_{n-1}$; $n = 1, 2, \ldots, N$; z_n is the coordinate of the bound between the nth and $(n+1)$th layers; and $\gamma_{N+1} = 0$. The transfer matrix for the wave with orthogonal polarization is obtained from Eq. (6) by changing h to $\sqrt{\varepsilon_{n-1}/\varepsilon_n}$. The transmittance, reflectance, and absorbance are given by the expressions

$$T(\omega) = \frac{1}{|\hat{M}_{11}|^2}, \quad R(\omega) = \frac{|\hat{M}_{11}|^2}{|\hat{M}_{21}|^2}, \quad (7)$$
$$A(\omega) = 1 - T(\omega) - R(\omega),$$

where $\hat{M}_{11}$ and $\hat{M}_{21}$ are the elements of the matrix $\hat{M}$.

3. RESULTS AND DISCUSSION

3.1. Optical Tamm Plasmon Polaritons at the Edge of the Photon Crystal Adjacent to the Isotropic Nanocomposite Layer

We first study optical Tamm states that are manifested in the form of standing surface waves at the interface between the photonic crystal and isotropic nanocomposite layer. The nanocomposite consists of metallic nanoballs dispersed in a dielectric matrix and is characterized by the effective complex permittivity $\varepsilon_{mix}(\omega)$, which is determined from Eq. (1) under the condition that $L_\perp = L_\parallel = 1/3$:

$$\varepsilon_{mix}(\omega) = \varepsilon'_{mix}(\omega) + i\varepsilon''_{mix}(\omega). \quad (8)$$

Neglecting the small coefficient γ^2 and using Eq. (1), we obtain the resonance frequency depending on the characteristics of the initial materials and the concentration of the disperse phase:

$$\omega_0 = \omega_p\sqrt{\frac{1-f}{3\varepsilon_d + (1-f)(\varepsilon_0 - \varepsilon_d)}}. \quad (9)$$

At the point $\omega = \omega_0$, the function $\varepsilon'_{mix}(\omega)$ vanishes and the function $\varepsilon''_{mix}(\omega)$ is maximal. The function $\varepsilon'_{mix}(\omega)$ also vanishes at the point

$$\omega_1 = \omega_p\sqrt{\frac{1+2f}{\varepsilon_0 + 2\varepsilon_d + 2f(\varepsilon_0 - \varepsilon_d)}}. \quad (10)$$

In the interval $[\omega_0, \omega_1]$, the function $\varepsilon'_{mix}(\omega)$ is negative, $\varepsilon'_{mix}(\omega) < 0$; i.e., the nanocomposite in this frequency range is similar to a metal.

A decrease in the field of the electromagnetic mode localized at the interface inside the nanocomposite is due to the negative permittivity of the nanocomposite ($\varepsilon'_{mix}(\omega) < 0$) at which the nanocomposite is similar to the metal. The decrease in the field inside the photonic

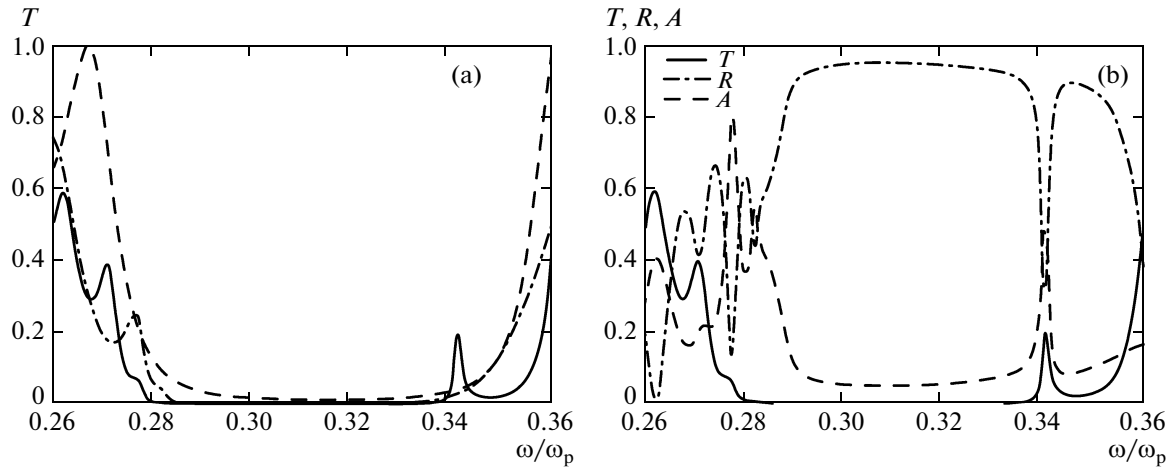

Fig. 3. (a) Transmission spectra at the normal incidence of light on the (dashed line) photonic crystal, (dash-dotted line) nanocomposite layer, and (solid line) photonic crystal adjacent to the nanocomposite layer. (b) Frequency dependences of the (solid line) transmittance T, (dashed line) reflectance R, and (dash-dotted line) absorbance at the normal incidence of light on the photonic crystal adjacent to the nanocomposite layer. The thickness of the nanocomposite layer is $d_{\text{mix}} = 150$ nm and the filling factor is $f = 0.2$.

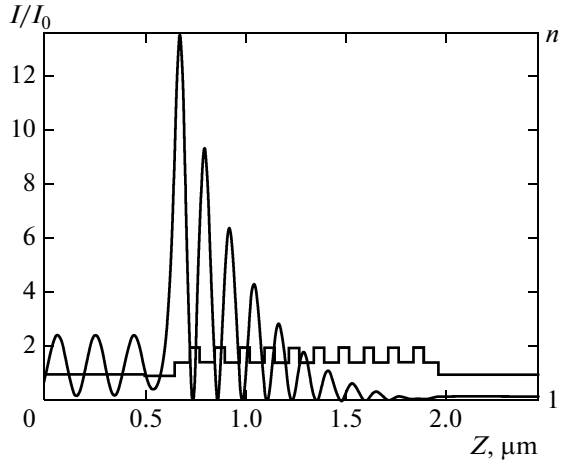

Fig. 4. Spatial distribution of the refractive index n and the field intensity divided by the input intensity for the case of the contact of the photonic crystal with the nanocomposite film. The thickness of the film is 150 nm and the filling factor is $f = 0.2$.

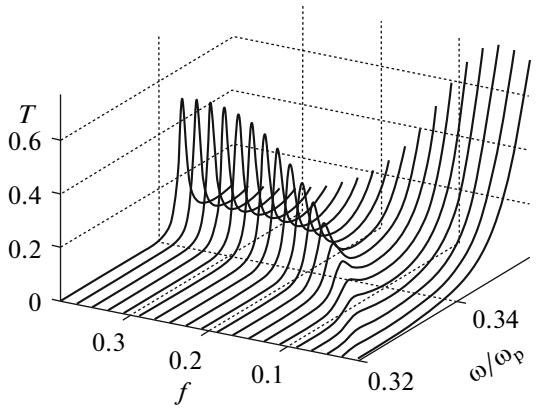

Fig. 5. Transmission spectra of the (photonic crystal–nanocomposite) system for various filling factors. The thickness of the nanocomposite layer is $d_{\text{mix}} = 100$ nm.

crystal is due to the damping of the Bloch wave at the frequency of the band gap or, in other words, to the Bragg reflection at the boundary of the periodic layered medium.

For definiteness, we consider zirconium dioxide (ZrO_2) with the permittivity $\varepsilon_b = 4.16$ and silicon dioxide (SiO_2) with the permittivity $\varepsilon_a = 2.10$ as the materials of alternating layers of the photonic crystal. The thicknesses of the respective layers are $d_b = 50$ nm and $d_a = 74$ nm and the number of layers is $N = 21$.

The dielectric layer of the nanocomposite with the thickness $d_{\text{mix}} = 150$ nm consists of silver nanoballs dispersed in transparent optical glass. For silver, $\varepsilon_0 = 5$, $\omega_p = 9$ eV, and $\gamma = 0.02$ eV; for glass, $\varepsilon_d = 2.56$. The frequency dependences of the real and imaginary parts of the permittivity calculated by Eq. (1) show that an increase in the volume concentration of nanoballs is accompanied by the shift of the frequency ω_0 corresponding to resonance in the defect layer toward lower frequencies. In this case, the half-width of the resonance curve $\varepsilon''_{\text{mix}}(\omega)$ changes only slightly, the curve $\varepsilon'_{\text{mix}}(\omega)$ is significantly modified, and the frequency

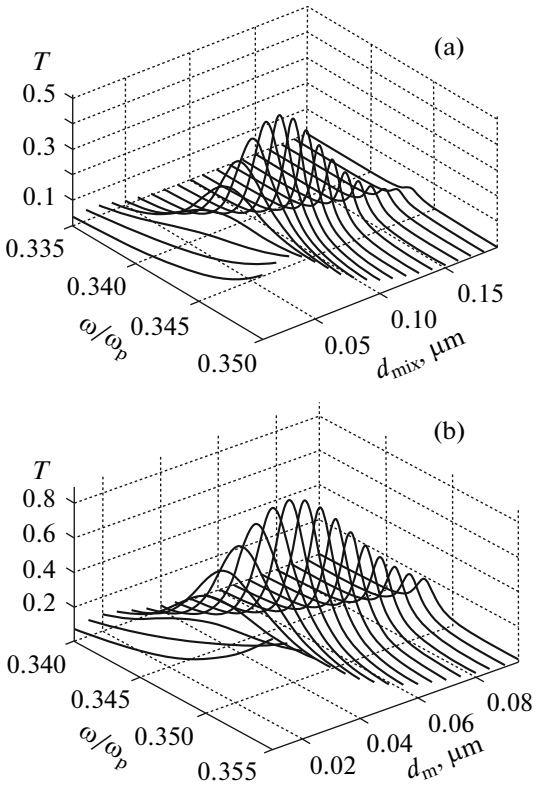

Fig. 6. Transmission spectra for various thicknesses of the (a) nanocomposite and (b) metal layers; $f = 0.3$ and 1.0 for the nanocomposite and silver layers, respectively.

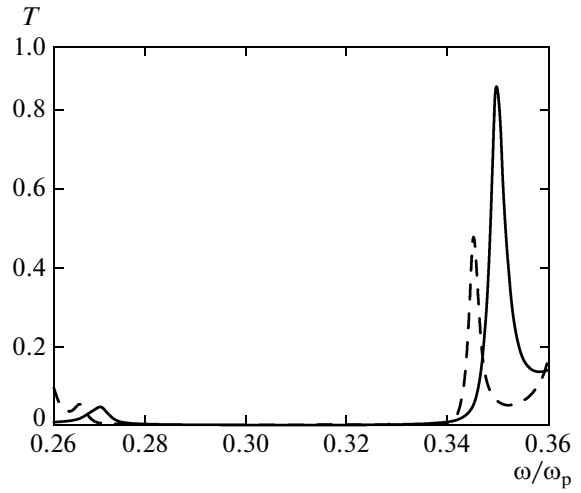

Fig. 7. Frequency dependence of the transmission spectra for the photonic crystal adjacent to the (dashed line) nanocomposite layer and (solid line) silver layer. For the nanocomposite layer, $d_{mix} = 100$ nm and $f = 0.3$; for the silver layer, $d_m = 50$ nm and $f = 1$.

range where $\varepsilon'_{mix}(\omega) < 0$ is expanded. For example, the dependences $\varepsilon'_{mix}(\omega)$ and $\varepsilon''_{mix}(\omega)$ for the filling factor $f = 0.2$ are shown in Fig. 2. Resonance observed at the frequency $\omega = 0.2882\omega_p$ with the corresponding wavelength $\lambda = 451.5$ nm is attributed to the plasmon resonance of nanoparticles [23, 26].

Figure 3a shows three transmission spectra at the normal incidence of light on the photonic crystal, nanocomposite layer, and photonic crystal adjacent to the nanocomposite layer. It is seen in this figure that the band gap of the nanocomposite significantly overlaps with the band gap of the photonic crystal and is obviously due to the absorption of light in the nanocomposite and to the existence of the frequency range where the nanocomposite is similar to a metal with the permittivity $\varepsilon'_{mix}(\omega) < 0$ (see Fig. 2). Furthermore, according to the figure, a passband corresponding to the Tamm state localized at the boundary of the photonic crystal adjacent to the nanocomposite appears near the upper edge of the band gap.

The found optical Tamm state exists only in a very narrow frequency range where the nanocomposite is similar to a metal (see inset in Fig. 2). The permittivity of the nanocomposite at the frequency of the Tamm state is

$$\varepsilon'_{mix}(\omega) = -0.8996 + 0.0882i.$$

At the same frequency, the permittivity of the silver film in the Drude approximation given by Eq. (4), which follows from Eq. (1) at the filling factor $f = 1$, is

$$\varepsilon = -3.6146 + 0.0562i.$$

Figure 3b shows the transmission, reflection, and absorption spectra for the (nanocomposite–photonic crystal) structure. Analysis of these spectra indicates that the energy conservation law (i.e., the condition $A(\omega) + R(\omega) + T(\omega) = 1$) is satisfied throughout the entire frequency range.

The distribution of the electric field intensity in the sample in the case of the contact of the photonic crystal with the nanocomposite film is illustrated in Fig. 4 for the frequency of the Tamm state. It is seen in the figure that the localized Tamm state is clearly manifested in the case of the use of the nanocomposite layer. The light field in the Tamm plasmon polariton is localized in the region comparative with the wavelength. However, in the case of the metal film with the same thickness and unchanged other parameters of the system, the Tamm state does not appear at the interface between the photonic crystal and sliver film.

The transmission spectrum of the photonic crystal structures under consideration is very sensitive to the filling factor of the nanocomposite. Figure 5 shows the transmission spectrum of the photonic crystal structure at a given thickness of the nano-

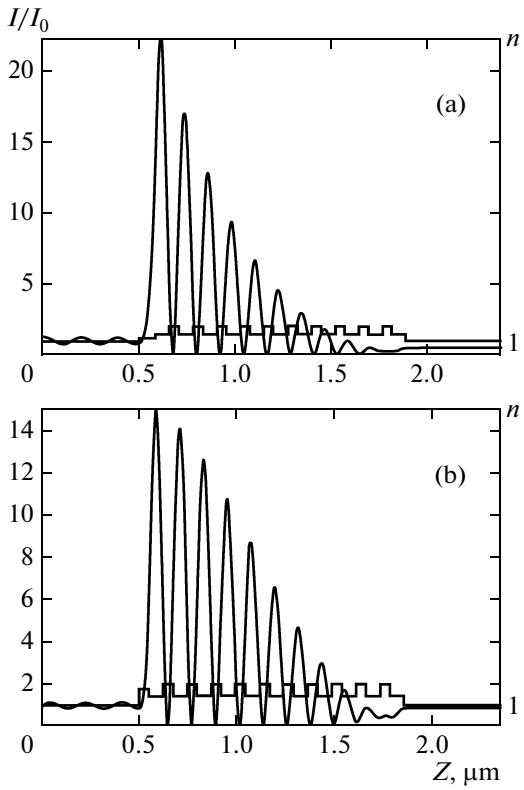

Fig. 8. Spatial distribution of the light field intensity and refractive index (a) for the (photonic crystal–nanocomposite) structure with $d_{mix} = 100$ nm and $f = 0.3$ and (b) for the (photonic crystal–silver layer) structure with $d_m = 50$ nm and $f = 1$.

composite layer and various filling factors f. According to the figure, an increase in the concentration of metallic nanoparticles results in the shift of the transmission peak of the corresponding optical Tamm state toward higher frequencies. The calculations show that an increase in the volume fraction of nanoballs from $f = 0.1$ to $f = 0.3$ leads to an increase in the maximum absolute value of the real part of the permittivity varying from -0.2962 to -1.4847; whereas the imaginary part of the permittivity remains almost unchanged. The localization length of the light field in the plasmon polariton also increases with the factor f. The localization length is defined as the distance from the boundary at which the envelope of the field intensity decreases by a factor of e.

Figure 6 shows the transmission spectra for photonic crystal structures at various thicknesses of the nanocomposite and silver layers with the factors $f = 0.3$ and 1.0, respectively.

For comparison, we consider the photonic crystal bounded by the nanocomposite film with the thickness $d_{mix} = 100$ nm and the photonic crystal bounded by the silver film with the thickness $d_m = 50$ nm. In this case, the transmittance of the (photonic crystal–nanocomposite) system at the frequency of the optical Tamm state is half of the transmittance of the (photonic crystal–silver film) system at the frequency of the optical Tamm state (Fig. 7). However, the maximum intensity of the light field in the localization region of the optical Tamm state at the interface between the photonic crystal and nanocomposite is twice as high as the maximum intensity of the Tamm mode at the interface between the photonic crystal and silver film, whereas the localization length in the former case is half of the localization length in the latter case (Fig. 8).

3.2. Coupled Tamm Plasmon Polaritons

In the case of the photonic crystal bounded from both sides by nanocomposite media, the transmission spectrum exhibits two passbands in the band gap of the photonic crystal.

Figures 9a and 9b show the transmission spectra of the photonic crystal structure for the cases where the nanocomposite film or silver film is located on one and two sides of the superlattice. In the case of the contact of the films with both sides of the photonic crystal, the optical Tamm modes localized at the interfaces overlap with each other, which leads to the lift of degeneracy; i.e., the frequency is split and two passbands appear in the transmission spectrum in the band gap of the photonic crystal.

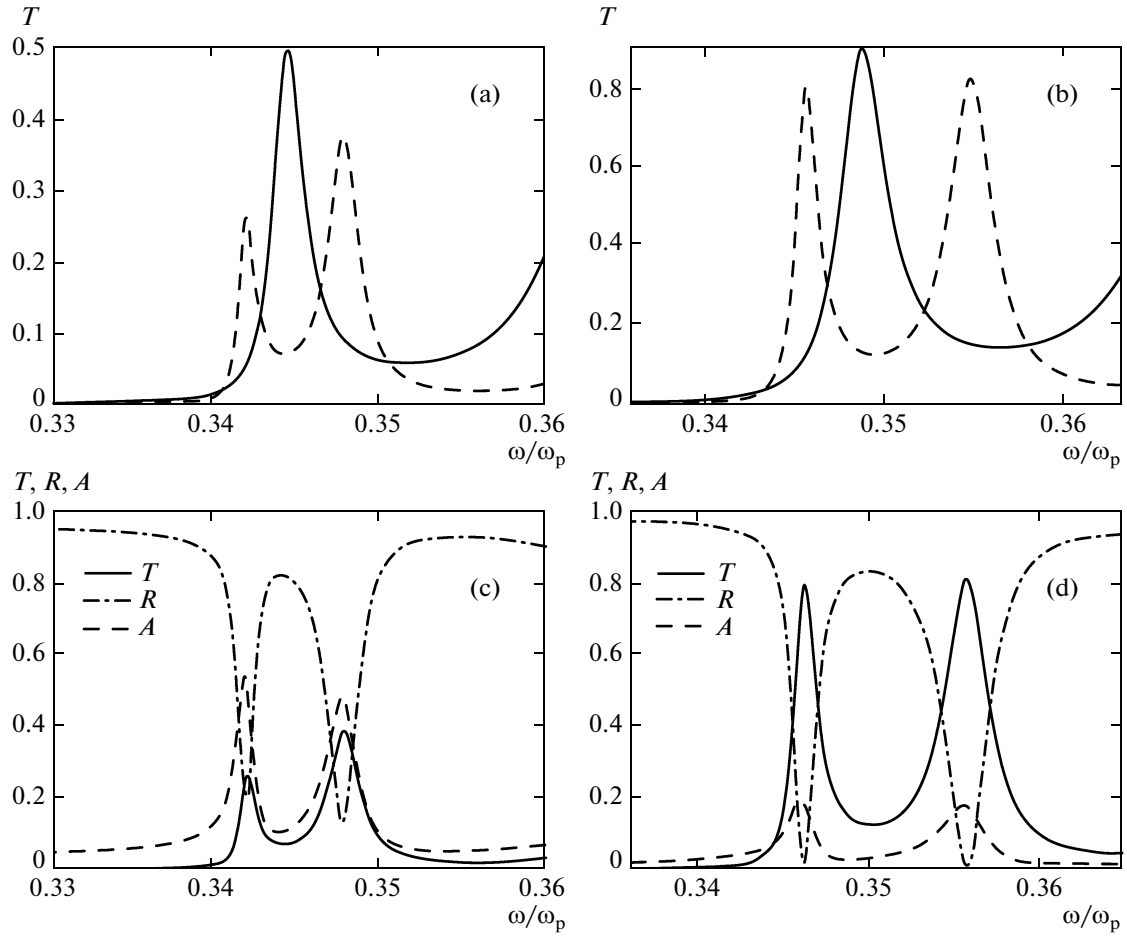

Fig. 9. Transmission spectra of the photonic crystal bounded from (solid lines) one side and (dashed lines) both sides by (a) nanocomposite and (b) metal media. The transmission, reflection, and absorption spectra of the photonic crystal bounded from both sides by (c) nanocomposite and (d) metal media. The thickness and filling factor of the nanocomposite are $d_{mix} = 100$ nm and $f = 0.3$, respectively; the thickness and filling factor of the silver film are $d_m = 50$ nm and $f = 1$, respectively.

The transmission, reflection, and absorption spectra of the photonic crystal bounded by the nanocomposite and metal films are shown in Figs. 9c and 9d.

The splitting of the frequency is approximately 6.7 and 10.6 nm for the photonic crystals bounded by the nanocomposite and silver films, respectively.

The distribution of the field for the case where the nanocomposite films are located on both sides of the photonic crystal is illustrated in Fig. 10 for the high- and low-frequency transmission peaks shown in Fig. 9a. It can be seen in Fig. 10 that coupling between Tamm plasmons localized at the interface between the photonic crystal and nanocomposite is responsible for the formation of symmetric and antisymmetric waveguide modes.

When the photonic crystal is bounded by silver films, the distribution of the electric field, as in [16], is similar to the distribution of the field in the symmetric and antisymmetric modes for the structure consisting of the photonic crystal bounded from both sides by nanocomposite films (Fig. 10).

3.3. Effect of the Shape of Nanoparticles in the Model of the Nanocomposite Medium

New features in the transmission spectrum appear in the case of Tamm optical states localized at the edge of the photonic crystal bounded by the anisotropic nanocomposite layer. In this case, the nanocomposite consists of spheroidal silver nanoparticles that are dispersed in the transparent glass matrix and are oriented along the axis of revolution coinciding with the x axis (Fig. 1). The technology for the fabrication of such nanocomposites with silver nanoparticles with the required shape and orientation in the glass matrix is known [27, 28]. Figure 11 shows the frequency dependences of the real and imaginary parts of the effective permittivities of the anisotropic nanocomposite medium as calculated by Eq. (1). It can be seen in the figure that the resonance frequencies depend on the direction of the electric field with respect to the axis of revolution of the spheroid and on the ratio of the lengths of the polar and equatorial semiaxes of the nanoparticles. Since the resonance frequencies of the

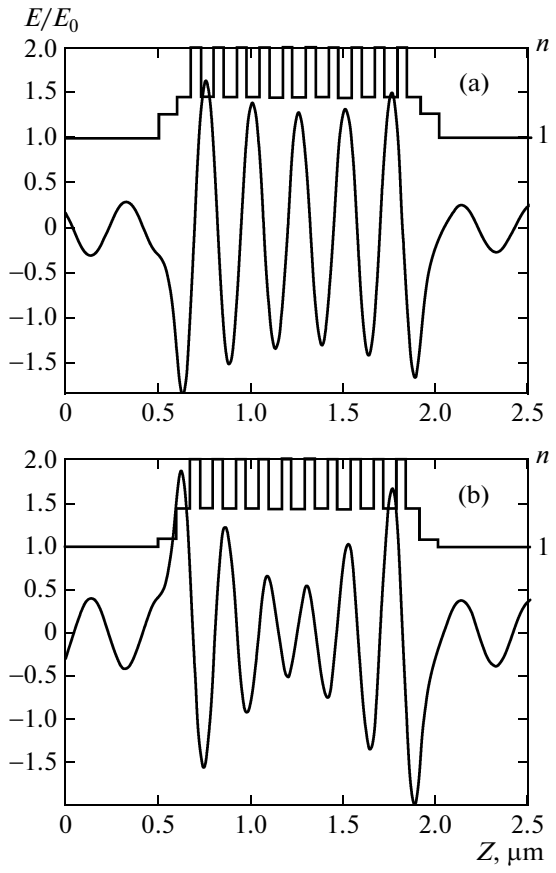

Fig. 10. Spatial distribution of the refractive index and electric field strength divided by the input strength for the (a) low-frequency symmetric and (b) high-frequency antisymmetric plasmon polariton modes of the structure. The thickness and filling factor of the nanocomposite are $d_{mix} = 100$ nm and $f = 0.3$, respectively.

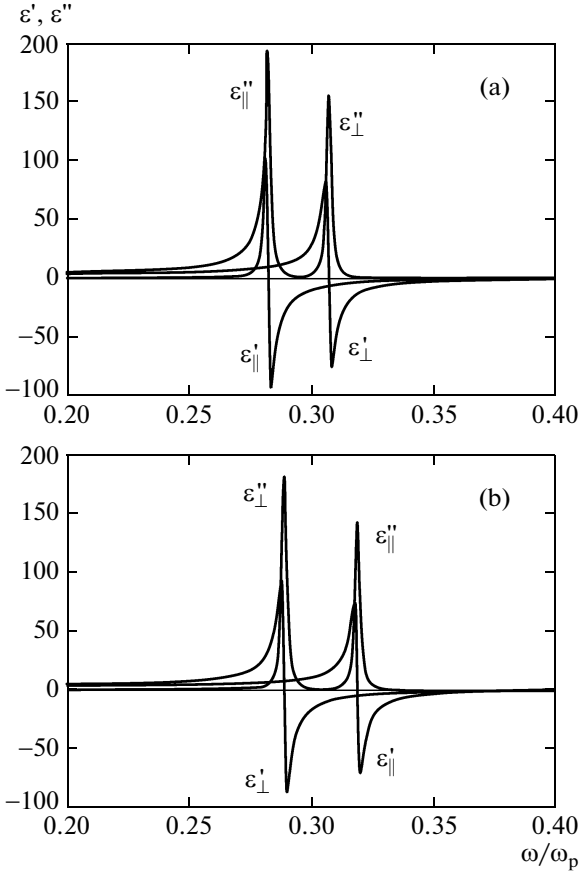

Fig. 11. Frequency dependences of the real ($\varepsilon'_\perp$, $\varepsilon'_\parallel$) and imaginary ($\varepsilon''_\perp$, $\varepsilon''_\parallel$) parts of the effective permittivity of the nanocomposite. The filling factor is $f = 0.2$ and the ratio of the lengths of the polar and equatorial semiaxes of the nanoparticle is $\xi =$ (a) 1.2 and (b) 0.8.

permittivities $\varepsilon_\perp$ and $\varepsilon_\parallel$ are different, the optical properties of the nanocomposite depend on the polarization of the incident wave.

The polarization sensitivity of the transmission spectrum is illustrated in Fig. 12, where it can be seen that the positions of the peaks of the optical Tamm state in the band gap depend on the polarization of the incident light and are 5.4 and 4.5 nm for the cases of (a) oblate and (b) prolate nanoparticles dispersed in the nanocomposite, respectively.

Figures 12c and 12d show the transmission, reflection, and absorption spectra for the perpendicular polarization of light for the oblate and prolate nanoparticles dispersed in the nanocomposite, respectively.

It is remarkable that, for both cases of oblate and prolate spheroidal nanoparticles dispersed in the nanocomposite, the degree of localization of Tamm states at the interface between the photonic crystal and nanocomposite increases with a decrease in the transmittance. In the case of oblate nanoparticles (see Fig. 12), the spatial distribution of the light field intensity in Tamm modes is shown in Fig. 13 for waves with the longitudinal and transverse polarizations.

The intensity at the maximum of the localized mode for *p* polarized waves (Fig. 13b) is by a factor of 3.6 higher than the intensity of transversely polarized waves (Fig. 13a). The difference between the respective intensities in the case of prolate spheroids is halved because the transmittances for waves with different polarizations are close to each other (see Fig. 12b).

4. CONCLUSIONS

Using the transfer matrix method, we have studied the spectral properties of the one-dimensional photonic crystal bounded from one or two sides by a resonantly absorbing layer of the nanocomposite, which consists of spherical or orientationally ordered spheroidal silver nanoparticles dispersed in transparent

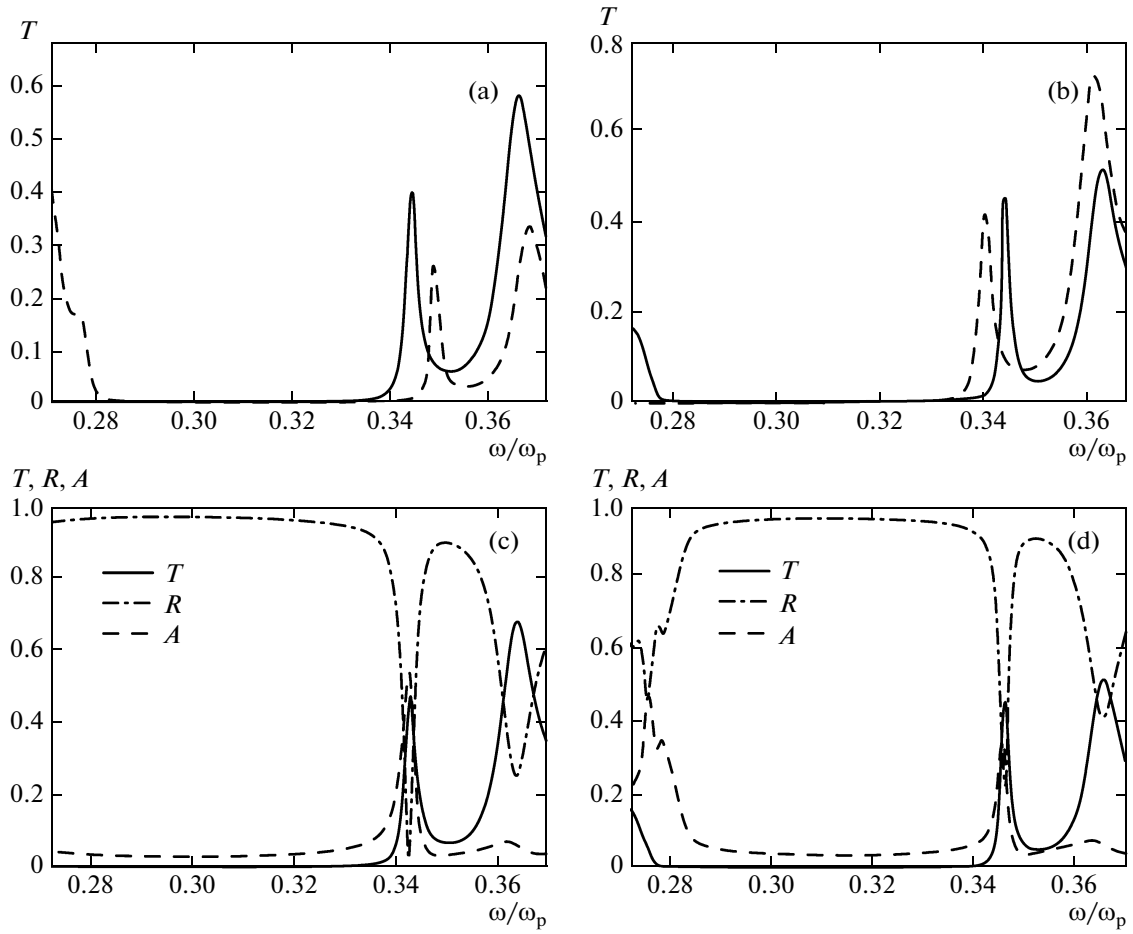

Fig. 12. Transmission spectra of the system for the (solid lines) perpendicular and (dashed lines) parallel (with respect to the optical axis of the nanocomposite) polarizations of light at $\xi =$ (a) 0.8 and (b) 1.2. The solid, dashed, and dash-dotted lines in panels (c, d) are the transmission, reflection, and absorption spectra, respectively, of the system for the perpendicular (with respect to the optical axis of the nanocomposite) polarization of light at $\xi =$ (a) 0.8 and (b) 1.2. The thickness and filling factor of the nanocomposite are $d_{\text{mix}} = 100$ nm and $f = 0.3$, respectively.

optical glass. The spectral manifestation of optical Tamm states, which is due to the presence of the frequency range, where the effective resonance permittivity of the nanocomposite is negative, in the visible spectrum has been revealed.

It has been shown that, at the normal incidence of light on the photonic crystal adjacent to the nanocomposite, the transmission spectrum has a peak inside the photonic band gap, which corresponds to the excitation of the optical Tamm state. The characteristics of the Tamm states localized at the edge of the photonic crystal are very sensitive to the volume fraction of nanoballs in the nanocomposite film and to its thickness. It has been shown that the frequency and degree of localization of Tamm states can be efficiently controlled by varying the volume fraction of nanoballs in the film of the nanocomposite, i.e., the thickness of the nanocomposite layer.

It has been shown that there are thicknesses of nanocomposite films at which the optical Tamm state is observed at the boundary of the photonic crystal adjacent to the nanocomposite, but the Tamm state does not appear if the photonic crystal is bounded by the silver film with the same thickness. The calculations have demonstrated that symmetric and antisymmetric waveguide modes in the photonic crystal bounded by the photonic crystal from both sides are formed because of coupling between Tamm plasmons localized at the interface between the photonic crystal and nanocomposite. It has been shown that, if the photonic crystal is adjacent to the anisotropic nanocomposite layer, the incident waves with the longitudinal and transverse polarizations correspond to individual plasmon resonance frequencies of the nanocomposite. Thus, the transmission spectrum exhibits two peaks in the photonic band gap of the photonic crystal,

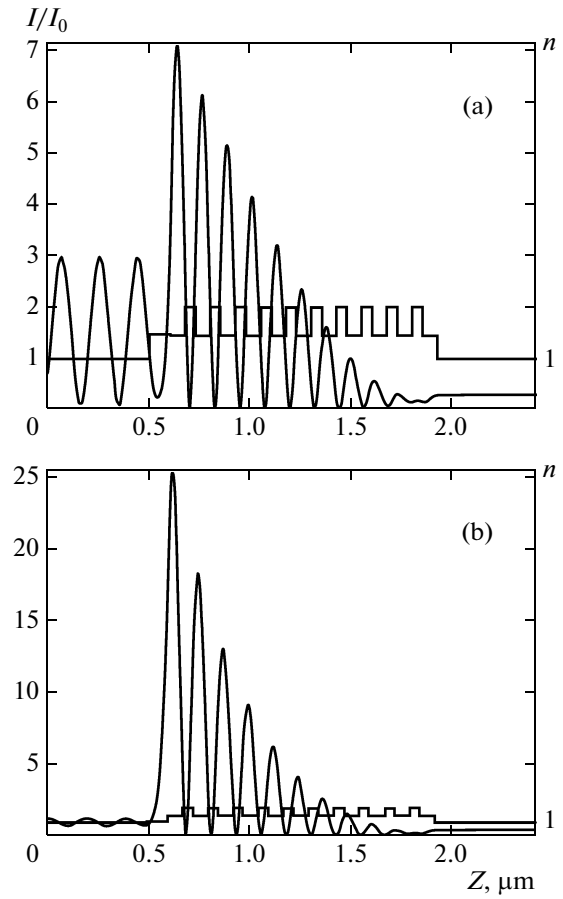

Fig. 13. Spatial distribution of the refractive index and electric field strength divided by the input strength for the (a) perpendicular and (b) parallel polarizations of light at the parameters $\xi = 0.8$, $f = 0.3$, and $d_{mix} = 100$ nm.

which correspond to the Tamm plasmons whose characteristics are very sensitive to the ratio of the lengths of the semiaxes of spheroidal nanoparticles.

ACKNOWLEDGMENTS

This work was supported by the Ministry of Education and Science of the Russian Federation (state contract no. 14.V37.21.0730, federal program "Human Capital for Science and Education in Innovative Russia"); by the Presidium of the Siberian Branch, Russian Academy of Sciences (project no. 24.29); by the Ministry of Education and Science of the Russian Federation (contract no. 14V37.21.0730); by the Division of Physical Sciences, Russian Academy of Sciences (project no. Sh.9.5); by the Presidium of the Russian Academy of Sciences (project nos. 24.29 and 24.31); and by the Siberian Branch, Russian Academy of Sciences (project nos. 43 and 101).

REFERENCES

1. J. D. Joannopoulos, S. G. Johnson, J. N. Winn, and R. D. Meade, *Photonic Crystals: Molding the Flow of Light* (Princeton University Press, Princeton, New Jersey, United States, 2008).
2. K. Sakoda, *Optical Properties of Photonic Crystals* (Springer-Verlag, Berlin, 2004).
3. K. Busch, S. Lölkes, R. B. Wehrspohn, and H. Föll, *Photonics Crystals: Advances in Design, Fabrication, and Characterization* (Wiley, Weinheim, 2004).
4. A. Yariv and P. Yeh, *Optical Waves in Crystals* (Wiley, New York, 1984).
5. A. P. Vinogradov, A. V. Dorofeenko, A. M. Merzlikin, and A. A. Lisyansky, Phys.—Usp. **53** (3), 243 (2010).
6. T. W. Ebbesen, J. Lezec, H. F. Ghaemi, T. Thio, and P. A. Wolff, Nature (London) **391**, 667 (1998).
7. F. G. Garcia-Vidal, L. Martin-Moreno, T. W. Ebbesen, and L. Kuipers, Rev. Mod. Phys. **82**, 729 (2010).
8. P. N. Melentiev, A. E. Afanasiev, A. A. Kuzin, A. V. Zablotskiy, A. S. Baturin, and V. I. Balykin, Opt. Express **19**, 22743 (2011).
9. P. N. Melentiev, A. E. Afanasiev, A. A. Kuzin, A. V. Zablotskiy, A. S. Baturin, and V. I. Balykin, J. Exp. Theor. Phys. **115** (2), 185 (2012).
10. I. V. Treshin, V. V. Klimov, P. N. Melentiev, and V. I. Balykin, arXiv:1305.4340v1 [physics.optics].
11. M. E. Sasin, R. P. Seisyan, M. A. Kalitteevski, S. Brand, R. A. Abram, J. M. Chamberlain, A. Yu. Egorov,

A. P. Vasil'ev, V. S. Mikhrin, and A. V. Kavokin, Appl. Phys. Lett. **92**, 251112 (2008).

12. W. L. Zhang and S. F. Yu, Opt. Commun. **283**, 2622 (2010).
13. T. Goto, A. V. Dorofeenko, A. M. Merzlikin, A. V. Baryshev, A. P. Vinogradov, M. Inoue, A. A. Lisyansky, and A. B. Granovsky, Phys. Rev. Lett. **101**, 113902 (2008).
14. H. Zhou, G. Yang, K. Wang, H. Long, and P. Lu, Opt. Lett. **35**, 4112 (2010).
15. A. Kavokin, I. Shelykh, and G. Malpuech, Appl. Phys. Lett. **87**, 261105 (2005).
16. I. Iorsh, P. V. Panicheva, I. A. Slovinskii, and M. A. Kaliteevski, Tech. Phys. Lett. **38** (4), 351 (2012).
17. S. G. Tikhodeev and N. A. Gippius, Phys.—Usp. **52** (9), 945 (2009).
18. P. N. D'yachenko and Yu. V. Miklyaev, Komp'yut. Opt. **31**, 31 (2007).
19. S. Ya. Vetrov, A. Yu. Avdeeva, and I. V. Timofeev, J. Exp. Theor. Phys. **113** (5), 755 (2011).
20. S. Ya. Vetrov, A. Yu. Avdeeva, R. G. Bikbaev, and I. V. Timofeev, Opt. Spectrosc. **113** (5), 517 (2012).
21. S. G. Moiseev, V. A. Ostatochnikov, and D. I. Sementsov, Kvantovaya Elektron. (Moscow) **42**, 557 (2012).
22. A. Oraevskii and I. Protsenko, Kvantovaya Elektron. (Moscow) **31**, 252 (2001).
23. A. Sihvola, *Electromagnetic Mixing Formulas and Applications* (Institution of Engineering and Technology, London, 2008).
24. L. A. Golovan, V. Yu. Timoshenko, and P. K. Kashkarov, Phys.—Usp. **50** (6), 595 (2007).
25. P. Yeh, J. Opt. Soc. Am. **69**, 742 (1979).
26. S. G. Moiseev, Opt. Spectrosc. **111** (2), 233 (2011).
27. D. Wang, S. Guo, and S. Yin, Opt. Eng. **42**, 3585 (2003).
28. S. D. Stookey and R. J. Aranjo, J. Appl. Opt. **7**, 777 (1968).

Translated by R. Tyapaev